

MODELLING THE EFFECTS OF DISTRIBUTED SERIES RESISTANCE ON SUNS- V_{oc} , m - V_{oc} AND J_{sc} -SUNS CURVES OF SOLAR CELLS

O. Kunz¹, S. Varlamov¹, and A.G. Aberle²

¹ Photovoltaics Centre of Excellence, The University of New South Wales, Sydney NSW 2052, Australia
Phone: +61 2 9385 4054, Fax: +61 2 9385 7762, E-mail: o.kunz@unsw.edu.au

² Solar Energy Research Institute of Singapore, National University of Singapore, Singapore 117576

ABSTRACT

A simple model based on the simulation of distributed series resistance effects in solar cells is presented. This model overcomes limitations of the standard two-diode model representation of solar cells in respect to fitting Suns- V_{oc} (m - V_{oc}) and J_{sc} -Suns curves. The model results include (i) an improved understanding of two-dimensional current flows in shunted solar cells, (ii) the prediction of shunt types from m - V_{oc} curves and corresponding distributed resistance model fits, (iii) the insight that lateral current flows in solar cells are responsible for deviations between J_{sc} -Suns data and two-diode model fits in the high illumination range. The presented approach extends the application range of Suns- V_{oc} measurements to solar cells which cannot adequately be described with the two-diode model.

INTRODUCTION

The two-diode model [1-4], which aims at describing the dark and illuminated I - V characteristics of p - n junction solar cells, is widely used to extract relevant device parameters such as the light-induced current density J_L , the shunt resistance R_{sh} , the lumped series resistance R_s and the saturation current densities J_{01} and J_{02} of the two diodes (D_1 and D_2) [1, 5-8]. Two-diode model fits to experimentally measured Suns- V_{oc} [9] curves are particularly useful since metal contacts are not required and the measurements can thus be performed during early stages of the cell fabrication sequence [6, 8].

However, in many cases this standard model is not sufficient to understand the characteristics of real devices due to non-idealities and three-dimensional current flows within the cells [2, 3, 10]. In this work we use a simple distributed series resistance (DSR) model to simulate Suns- V_{oc} , m - V_{oc} and J_{sc} -Suns [7] curves. We show that the presented DSR model is able to explain deviations between measured and two-diode modelled data that are frequently observed in these measurements.

THE DISTRIBUTED SERIES RESISTANCE MODEL

The DSR model used in this work comprises n identical unit solar cells D_i (Fig. 1(a)) in a parallel arrangement (Fig. 1(c, d)). Each unit solar cell conforms with the two-diode model representation with the exception of the additional resistors $R_{s,BSF,i}$ and $R_{s,em,i}$ that form the interconnections to adjacent unit solar cells

and/or the external elements. The two-diode model parameters used for the unit solar cells are obtained via Suns- V_{oc} measurements. To model Suns- V_{oc} measurements we adapted the equivalent circuit diagram (Fig. 1(c)) to represent the contacting structure used by our group (Fig. 1(b)). Note that for contact induced shunting the current flow is predominantly perpendicular to the grid fingers, while for J_{sc} -Suns measurements the main current flow is along the grid fingers (right rectangle Fig. 1(b)). Therefore, the equivalent circuit model for J_{sc} -Suns fitting has the external contacts at the opposing ends (Fig. 1(d)). The resistances that are related to the back surface field (BSF) and the emitter layer are lumped into two parameters $R_{s,BSF}$ and $R_{s,em}$, respectively, whereby

$$R_{s,BSF} = 2n \times R_{s,BSF,i} \quad \text{and} \quad R_{s,em} = 2n \times R_{s,em,i} \quad (1)$$

Equivalent equations hold for R_{sh} , J_L , and the diode saturation currents J_{01} and J_{02} , respectively. The actual device modelling is carried out using the circuit simulating software LT-Spice [11]. We found that a model comprising $n = 8$ identical unit solar cells is sufficient to adequately describe the measured data and thus to resolve the discrepancies between the experimental data and the two-diode model fits observed for many of our thin-film cells.

It should be noted that it is helpful, but not necessary, to understand the current flow in a particular solar cell structure. The DSR model accounts for the fact that different regions of the solar cell are biased differently when in operation. It is not essential to know where on the cell regions of identical bias conditions are located in order to obtain useful model results. In this paper the DSR model is used to model poly-Si thin-film solar cells. However, the model is by no means restricted to this type of solar cell.

RESULTS

(A) Suns- V_{oc} and m - V_{oc} results of shunted solar cells

Suns- V_{oc} curves are routinely used to identify diode properties such as open-circuit voltage, pseudo fill factor, diode ideality factors, etc., and to discern the effects of bulk and depletion region recombination [8]. Since Suns- V_{oc} curves are pseudo I - V curves, they allow for extraction of the local ideality factor m [12] using

$$m(V_{oc}) \cong \frac{1}{V_T} \left(\frac{\Delta V_{oc}(\Phi)}{\Delta(\ln(\Phi))} \right), \quad (2)$$

where $\Delta V_{oc}(\Phi)$ is the difference in open-circuit voltage, and $\Delta(\ln(\Phi))$ denotes the difference of the logarithms of the corresponding light intensities Φ (in *Suns*) between two subsequent data points. Analyzing m - V_{oc} curves has the advantage that subtle details often become apparent which cannot be noticed when looking at the original $Suns$ - V_{oc} curves. Local ideality factors determined from $Suns$ - V_{oc} curves at 1 Sun illumination were previously used by Bowden et al. [13] to identify junction recombination in wafer based Si solar cells.

In Fig. 2 general trends of $Suns$ - V_{oc} (a, c) and m - V_{oc} curves (b, d) are displayed whereby the DSR model features a resistive (a, b) or diode-like (c, d) shunt at the emitter finger (dashed oval in Fig. 1(c)). Note that the used DSR model is highly versatile and that it was altered to correspond to the particular cell structure and metallisation pattern used by our group (see Figs. 1(b) and (c)).

Resistive shunting is frequently present in solar cells. In the case of thin-film solar cells resistive shunting can be introduced, for example, if the metal electrodes (emitter or BSF) form ohmic contacts between the heavily doped layers of the cell. The situation of an ohmic shunt at the emitter finger is modelled in Figs. 2(a, b) where the diode parameters of a non-metallised silicon thin-film solar cell (determined via $Suns$ - V_{oc}) were used as a starting point for the DSR model. Note that these virgin $Suns$ - V_{oc} data are added to Fig. 2 for comparison (open

diamonds). A resistive shunt was added to the model with successively decreasing resistance values ($R_{sh} = \infty, 4000, 1000, 400$ and $100 \Omega\text{cm}^2$). In all cases a solar cell area of 1 cm^2 was modelled and BSF and emitter sheet resistance values were assumed to be $1000 \Omega/\square$ and $200 \Omega/\square$, respectively. These are realistic values for the heavily doped layers of our solar cells.

In Fig. 2(a) it can be seen that the $Suns$ - V_{oc} curves remain unchanged in the high illumination regime (> 2 *Suns*). However they deviate significantly in the lower illumination regime when compared to the virgin case. The 1-Sun V_{oc} only gets affected in the severe case of $R_{sh} = 100 \Omega\text{cm}^2$ where it drops from originally about 430 mV to 400 mV. This indicates that quite substantial linear shunting is necessary in order to cause a significant decrease in V_{oc} . From Fig. 2(b) it can be seen that decreasing the shunt resistance leads to the evolution of a hump in the m - V_{oc} curve in the low-voltage regime, whereby the peak becomes successively higher and the hump more pronounced when the shunt resistance decreases. The peak of the hump shifts towards higher voltages with decreasing shunt resistance values but is, in all cases, located at voltages below 300 mV.

In the case of non-linear shunting, both $Suns$ - V_{oc} and m - V_{oc} curves get affected in a completely different way. The shunting element used in this case is a diode with an ideality factor $n_{sh} = 1.1$, resembling a Schottky-type shunt introduced by the emitter metal finger.

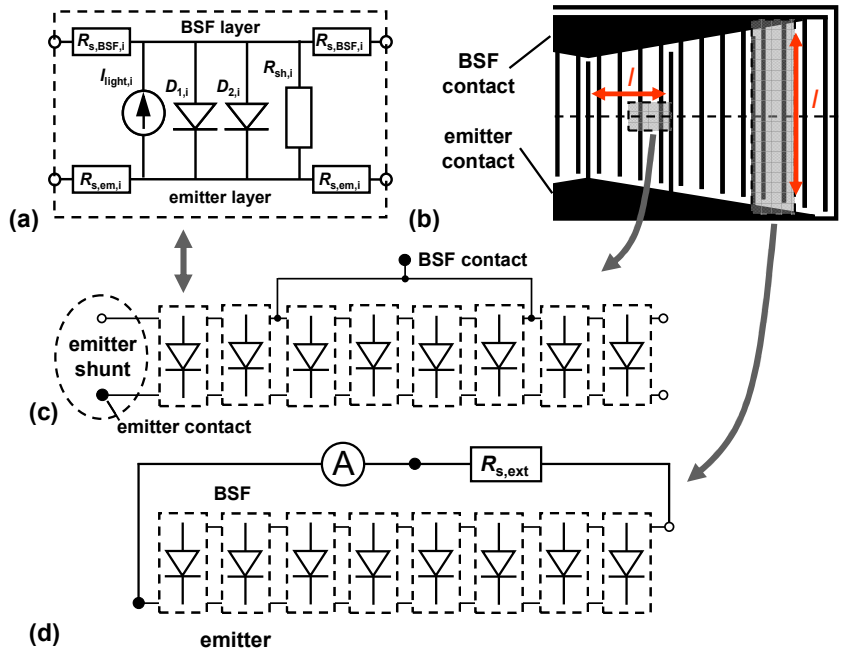


Fig. 1. (a) Equivalent circuit diagram of the unit solar cell; (b) simplified schematic of the contact structure used in our lab; (c) DSR model for $Suns$ - V_{oc} , and m - V_{oc} curves; (d) DSR model for J_{sc} - $Suns$ curves.

Note that the grey rectangles in (b) correspond to the circuits shown in (c) and (d). The red arrows indicate the predominant current flow direction.

It should be noted that Schottky diodes are generally quoted to have diode ideality factors slightly above unity and reverse saturation current densities orders of magnitude higher than observed for of p - n junction diodes [14]. The reverse saturation current densities $J_{0,sh}$ used in the following simulation have values from 10^{-6} to 10^{-3} mA/cm², increasing in steps of one decade.

Figure 2(c) presents the resulting Suns- V_{oc} curves. It can be seen that severe distortions already occur for $J_{0,sh}$ values of 10^{-5} mA/cm². In contrast to the resistive case, the deviation of the modelled Suns- V_{oc} curves from the undisturbed case is first seen at higher illumination levels, where the curves develop an unusual convex shape with increasing $J_{0,sh}$ values. Note that the 1-Sun V_{oc} reduces significantly with increasing $J_{0,sh}$ and drops below 300 mV in the case of $J_{0,sh} = 10^{-3}$ mA/cm² (originally V_{oc} was about 430 mV). The m - V_{oc} curves presented in Fig. 2(d) show that the additional Schottky diode results in a significant decrease of the local ideality factor at low voltages. With increasing $J_{0,sh}$ a bump evolves, located at significantly higher voltages than in the resistive case. The maximum m value is clearly greater than two. Increasing $J_{0,sh}$ moves the hump to lower voltages, but in contrast to the resistive case its location stays well above 300 mV in all modelled scenarios.

Additionally, the effect of the layer resistance on the Suns- V_{oc} and m - V_{oc} curves was investigated. It was found that a change in sheet resistance has little impact on the resistive case even if zero resistances are used. If the layer resistances are set to zero, the DSR model reduces to the standard two-diode model. Therefore the DSR model offers little benefit to modelling solar cells that feature purely ohmic shunts. In the case of a diode-like emitter shunt the sheet resistance impacts mainly the peak voltage of the hump in the m - V_{oc} curve.

A comparison between measured and modeled Suns- V_{oc} and m - V_{oc} curves of a metallised poly-Si thin-film solar cell is shown in Figs. 3(a) and 3(b), respectively. Note that the Suns- V_{oc} parameters of the non-metallised diode ("virgin data") were used as basis for the DSR model and that the external shunt was subsequently adjusted to obtain the best possible fit. A remarkably good agreement between measured and modeled data was achieved using a diode shunt with $n_{sh} = 1.8$ and $J_{0,sh} = 2 \times 10^{-5}$ A/cm². From the location of the hump on the m - V_{oc} curve (> 300 mV) and the particular DSR model fit it can be concluded that non-linear (i.e., diode-like) shunting is an important loss mechanism in this particular solar cell.

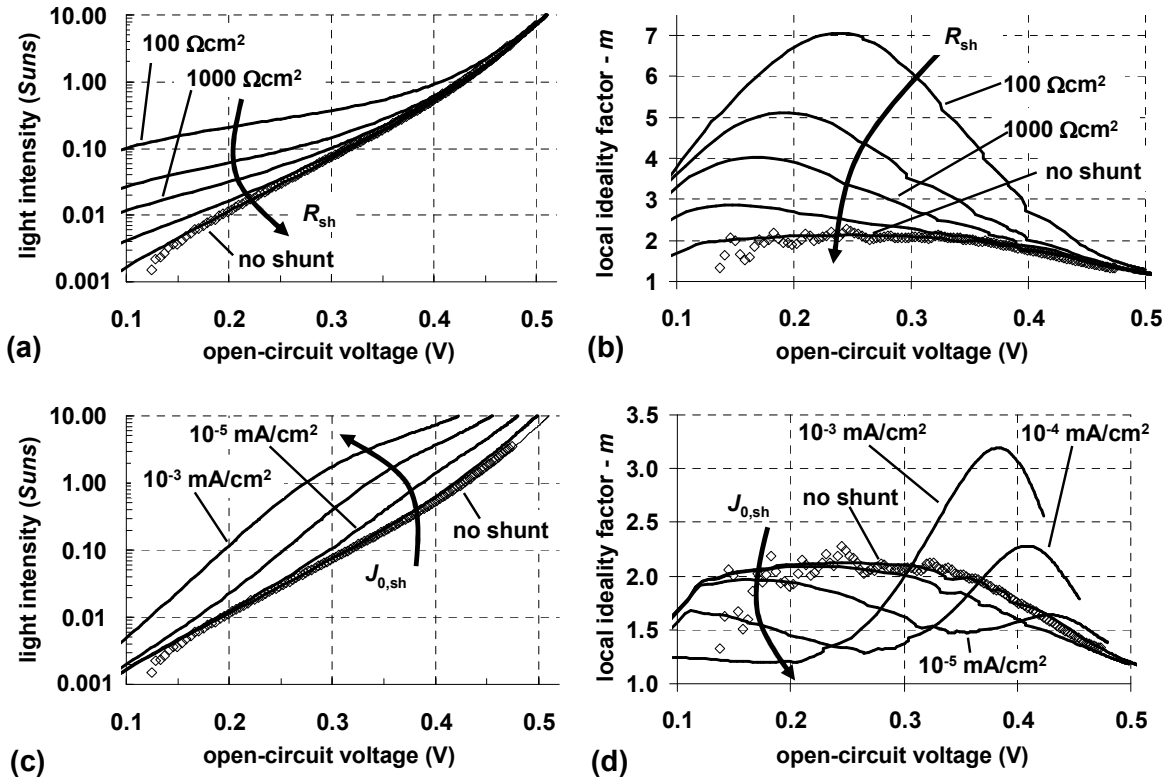


Fig. 2. (a, b) Comparison between experimental data (open diamonds, no shunting) and modelled curves (solid lines) for R_{sh} values ranging from infinity (no shunt) to $100 \Omega\text{cm}^2$. (a) Suns- V_{oc} curves; and (b) m - V_{oc} curves. (c, d) Comparison between experimental data (open diamonds, no shunting) and modelled curves (solid lines) when the saturation current density of the shunting diode $J_{0,sh}$ is varied from 10^{-6} to 10^{-3} mA/cm². (a) Suns- V_{oc} curves; and (d) m - V_{oc} curves.

This finding agrees well with microscopic images and lock-in thermographic images of this solar cell clearly revealing shunting between the emitter grid lines and the adjacent absorber layer. We relate the high ideality factor that was necessary in order to get a satisfactory DSR model fit to defect recombination at the Schottky interface. Note that high ideality factors of around 1.8 (generally between 1 and 2) are expected for p - n junction diodes that feature a high defect density in the junction's depletion region such as is the case for polycrystalline material [15, 16].

(B) J_{sc} -Suns results

J_{sc} -Suns measurements in combination with two-diode model fits have previously been shown to be useful for the determination of the light-induced current density and the series resistance of crudely metallised thin-film solar cells (mesa type devices) [7]. However, when this technique is applied to fully metallised solar cells we found that the fit quality is often significantly compromised compared to the case of mesa-type cells [17]. Therefore the determination of the lumped series resistance is only possible within certain boundaries.

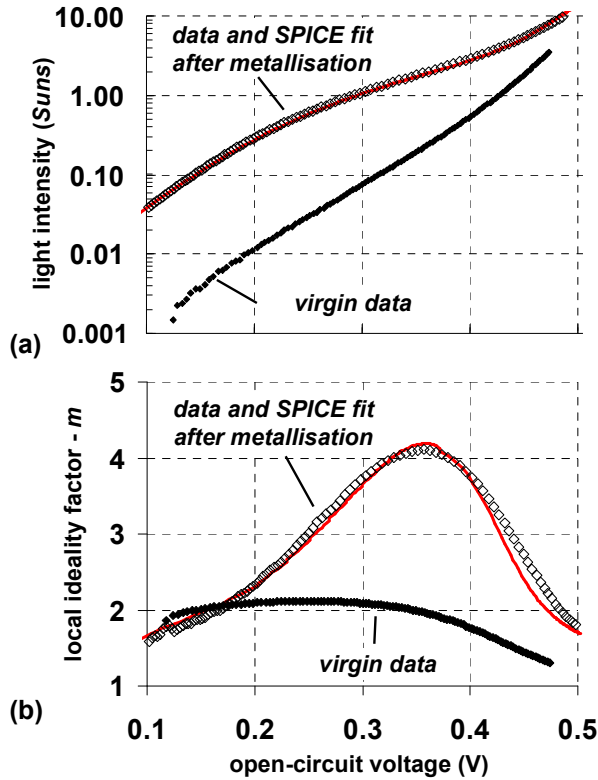


Fig. 3. Comparison between experimental data (open diamonds) and DSR model fit (solid line) of a Si thin-film solar cell featuring Schottky-type shunting. (a) Suns- V_{oc} curves; and (b) m - V_{oc} curves. The data of the non-metallized, non-shunted cell (filled diamonds; “virgin data”) are added for comparison.

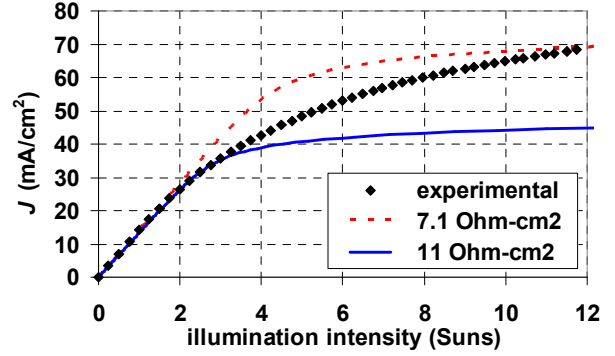


Fig. 4. Comparison between experimental data (diamonds) and two-diode model fits with $J_L = 15.6 \text{ mA/cm}^2$, $R_s = 7.1 \text{ } \Omega\text{cm}^2$ (dashed red line) and $R_s = 11 \text{ } \Omega\text{cm}^2$ (solid blue line).

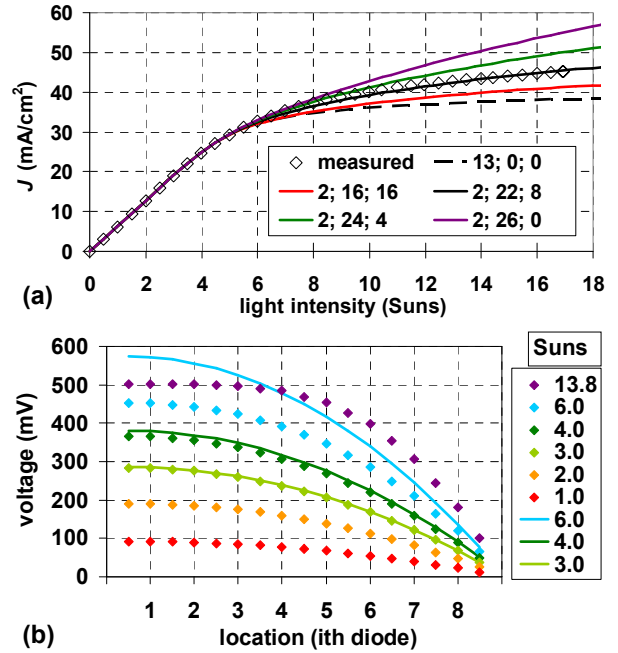


Fig. 5. (a) Comparison between two-diode model fit (dashed line), DSR model fits (solid lines) and experimental J_{sc} -Suns data (open diamonds) of a metallised Si thin-film solar cell. The two-diode model parameters that were used are: $I_L = 6.4 \text{ mA}$, $I_{01} = 2.36 \times 10^{-10} \text{ A}$, $I_{02} = 1.31 \times 10^{-6} \text{ A}$. The DSR model parameters displayed in the legend are: $R_{s,ext}$; $R_{s,BSF}$; $R_{s,em}$. (b) Voltage distribution as a function of location on the DSR model for different light intensity values (in Suns, see legend). Note that the number on the x-axis corresponds to the diodes of the i^{th} unit solar cell with respect to the model displayed in Fig. 1(d). The DSR model parameters are: $R_{s,ext} = 2 \text{ } \Omega$, $R_{s,BSF} = 26 \text{ } \Omega$, $R_{s,em} = 0$. Voltages for an equivalent purely resistive network are added (solid lines) for light intensities of 3, 4, and 6 Suns, respectively.

This is illustrated in Fig. 4 where experimental J_{sc} -Suns data of a fully metallised Si thin-film solar cell are displayed. It can be seen that the two-diode model fits that were added for comparison do not adequately represent the experimental data.

To improve our understanding of the failure of the two-diode model fits to J_{sc} -Suns data, Fig. 5(a) displays DSR model fits to J_{sc} -Suns data whereby R_{ext} (see Fig. 1(d)) was kept at 2Ω and the ratio of $R_{s,BSF}$ to $R_{s,em}$ was varied. In all cases the DSR model is superior to the standard two-diode model. It is evident that an excellent fit of the experimental data was achieved with the DSR model parameters $R_{s,BSF} = 22 \Omega$ and $R_{s,em} = 8 \Omega$.

Figure 5(b) displays the bias voltage at the i^{th} diode of the DSR model ($R_{s,ext} = 2 \Omega$, $R_{s,BSF} = 26 \Omega$, $R_{s,em} = 0$) for a given illumination intensity. The standard two-diode model fit assumes that all diodes within the solar cell have the same bias condition. In contrast, Fig. 5(b) shows that this is not the case for the DSR model at any illumination intensity. To illustrate the influence of the diodes on the bias voltages we also display the analytically calculated voltage distribution of the DSR model (corresponding to the DSR model when the diodes are removed). In the presented case the influence of the diodes can be seen at illumination intensities of ≥ 4 Suns. At high illumination intensities the voltage distribution consists essentially of two regions: a region of constant potential and a transition region where the bias voltages reduce to the contact potential.

CONCLUSIONS

Suns- V_{oc} curves of fully metallised solar cells can, in many cases, not be adequately fitted with the standard two-diode model. Modeling of the distributed series resistance of solar cells has been shown to overcome and explain these limitations. This was demonstrated for the case of linear and non-linear shunting at the emitter line contacts of poly-Si thin-film solar cells. It was demonstrated that both Suns- V_{oc} and m - V_{oc} curves of these cells show significant deviations from the non-shunted curves when resistive or diode-like shunting is present at the emitter contacts. In both cases bumps evolve in the m - V_{oc} curves. For resistive shunts these bumps occur at voltages below 300 mV and for diode-like (Schottky) shunts they develop at voltages above 300 mV. Adjusting the sheet resistances of the heavily doped layers in the DSR model has a significantly larger effect in the case of non-linear shunts than for ohmic shunts. Therefore, employing the DSR model was found to be unnecessary for ohmic shunts.

An excellent fit to the measured data of a diode-shunted solar cell was obtained using the presented model, demonstrating its usefulness and validity.

While these investigations were tailored to poly-Si thin-film solar cells and the aligned bifacial metallisation scheme currently used at UNSW, the model is very versatile and can be applied to a large variety of solar cell types, metallisation schemes and shunting scenarios.

J_{sc} -Suns curves of fully metallised Si thin-film solar cells cannot be fitted satisfactorily using the standard two-

diode model. Through modeling of the distributed series resistance it was possible to show that the distributed nature of R_s and the corresponding multidimensional current flows are responsible for this effect. Despite the fact that the model is still only an approximation to the real behavior of the solar cell, it has value in that it allows a much better description of the J_{sc} -Suns curves than the standard two-diode model.

Further work is necessary to quantify the relationship between the DSR model results presented here and lumped R_s results obtained by other methods, given different possible solutions of the DSR model for experimental J_{sc} -Suns data.

ACKNOWLEDGEMENTS

OK acknowledges his PhD scholarship from The University of New South Wales (UNSW). The Photovoltaics Centre of Excellence at UNSW is one of the Centres of Excellence established and supported by the Australian Research Council (ARC). The Solar Energy Research Institute of Singapore (SERIS) is supported by the Singapore Government and the National University of Singapore.

REFERENCES

- [1] J. Zhao, A. Wang, P. Altermatt, and M.A. Green, "18.2% efficient multicrystalline silicon cell," in Proc. of the 26th IEEE Photovoltaic Specialists Conference, Anaheim, CA, USA, 1997, pp. 227-230.
- [2] A.S.H. Van der Heide, A. Schoenecker, J.H. Bultman, and W.C. Sinke, "Explanation of High Solar Cell Diode Factors by Nonuniform Contact Resistance," *Progress in Photovoltaics: Research and Applications*, vol. 13, pp. 3-16, 2005.
- [3] K.-I. Kurobe, and H. Matsunami, "New two-diode model for detailed analysis of multicrystalline silicon solar cells," *Japanese Journal of Applied Physics, Part 1: Regular Papers and Short Notes and Review Papers*, vol. 44, pp. 8314-8321, 2005.
- [4] M. Wolf, and H. Rauschenbach, "Series resistance effects on solar cell measurements," *Advanced Energy Conversion*, vol. 3, pp. 455-479, 1963.
- [5] J.P. Charles, G. Bordure, A. Khoury, and P. Mialhe, "Consistency of the Double Exponential Model with the Physical Mechanism of Conduction for a Solar Cell under Illumination," *Journal of Physics D: Applied Physics*, vol. 18, pp. 2261-2268, 1985.
- [6] M.J. Keevers, A. Turner, U. Schubert, P.A. Basore, and M.A. Green, "Remarkably Effective Hydrogenation of Crystalline Silicon on Glass Modules," in Proc. of the 20th European Photovoltaic Solar Energy Conference, Barcelona, Spain, 2005, pp. 226-229.

- [7] O. Kunz, D. Inns, A.B. Sproul, and A.G. Aberle, "Application of Suns-Voc and Jsc-Suns measurements to the characterization of mesa-type thin-film solar cells," in Proc. of the *21st European Photovoltaic Solar Energy Conference*, Dresden, Germany, 2006, pp. 374-377.
- [8] S. Irwan Sulaiman, "Analysis of fitted Suns-Voc curves using two-diode model," in Proc. of the *IEEE International Conference on Semiconductor Electronics*, 2004, p. 6.
- [9] R.A. Sinton, and A. Cuevas, "A Quasi-Steady-State Open-Circuit Method for Solar Cell Characterization," in Proc. of the *16th European Photovoltaic Solar Energy Conference*, Glasgow, Scotland, 2000, pp. 1152-1155.
- [10] B. Galiana, C. Algora, I. Rey-Stolle, and I. Garcia Vara, "A 3-D model for concentrator solar cells based on distributed circuit units," *IEEE Transactions on Electron Devices*, vol. **52**, pp. 2552-2558, 2005.
- [11] Linear Technology, "LT Spice Users Guide," available at: <http://ltspice.linear.com/software/scad3.pdf>.
- [12] K. McIntosh, "Lumps, humps, and bumps: Three detrimental effects in the current-voltage curve of silicon solar cells," University of New South Wales, Sydney, PhD thesis, January 2001.
- [13] S. Bowden, V. Yelundur, and A. Rohatgi, "Implied-Voc and Suns-Voc Measurements in Multicrystalline Solar Cells," in Proc. of the *29th IEEE Photovoltaic Specialists Conference*, New Orleans, USA, 2002, pp. 371-374.
- [14] R.S. Muller, T.I. Kamins, and M. Chan, *Device Electronics for Integrated Circuits (3rd edition)*. New York: John Wiley and Sons, 2003.
- [15] S.A. Edmiston, G. Heiser, A.B. Sproul, and M.A. Green, "Improved modeling of grain boundary recombination in bulk and p-n junction regions of polycrystalline silicon solar cells," *Journal of Applied Physics*, vol. **80**, p. 6783, 1996.
- [16] J. Pallares, L.F. Marsal, X. Correig, J. Calderer, and R. Alcubilla, "Space charge recombination in P-N junctions with a discrete and continuous trap distribution," *Solid-State Electronics: An International Journal*, vol. **41**, pp. 17-23, 1997.
- [17] O. Kunz, "Evaporated Solid-phase Crystallised Polysilicon Thin-film Solar Cells on Glass," University of New South Wales, Sydney, PhD thesis, 2009.